

The physical vulnerability of different types of building structure to debris flow events

Hyo-sub Kang¹ · Yun-tae Kim¹

Received: 7 April 2015 / Accepted: 10 October 2015 / Published online: 15 October 2015
© Springer Science+Business Media Dordrecht 2015

Abstract Vulnerability assessment of elements at risk is a key component for risk assessment. The representative element at risk for debris flow is a residential building in downstream mountain, and the physical vulnerability of such a building depends on the structural characteristics of a building. The main objective of this paper was to construct physical vulnerability curves for different types of building structures in Korea to enable a quantitative assessment of debris flow risks. The physical characteristics of debris flows were analyzed based on 11 debris flow events that occurred in July and August, 2011. A total of 25 buildings that were damaged during these events were investigated in detail to determine the characteristics and patterns of damage. This study analyzes the relationship between the degree of building damage and the intensity of the debris flows through field survey data, spatial data, and empirical formula. Three different empirical vulnerability curves were obtained as functions of the debris flow depth, the flow velocity, and the impact pressure. Furthermore, the vulnerability function was characterized according to the structural type of the buildings. In the case of non-RC buildings, complete destruction occurred with an impact pressure greater than 30 kPa. For RC buildings, slight damage occurred with impact pressures less than 35 kPa. The impact pressure of debris flows corresponding to slight damage to RC buildings could result in complete destruction of non-RC buildings. The physical vulnerability curves suggested here have potential applications in quantitative assessment of the structural resistance of buildings to debris flow events.

Keywords Building damage · Structural type · Vulnerability function · Impact pressure · Debris flow

✉ Yun-tae Kim
yuntkim@pknu.ac.kr

Hyo-sub Kang
monkle0@hanamail.net

¹ Department of Ocean Engineering, Pukyong National University, Busan, South Korea

1 Introduction

The continued increase in population and resulting demand for resources has given rise to pressures to settle in places where continuous land development processes become a risk (Nadim and Kjekstad 2009). Human lives and structures located in debris flow-prone mountainous areas are commonly subject to debris flow hazards (Hu et al. 2012). In such areas, the development of appropriate hazard mitigation plans is an important aspect of public administration and civil protection (Zanchetta et al. 2004). In recent decades, many debris flow disasters have been reported in locations across the world. Previous research into debris flows has mainly focused on landslide hazard mapping and the corresponding triggering mechanisms (Van Westen et al. 2003; Sassa et al. 1997; Iverson 1997); however, there is an increasing interest in researches on risk assessment (Papathoma-Köhle et al. 2012, 2015; Totschnig and Fuchs 2013). For a risk assessment, vulnerability assessment for the elements at risk in debris flow is required.

Elements that are exposed to debris flow hazards include buildings, highways, railways, mines, and reservoirs. Compared with structural facilities such as railway bridges, common residential buildings are more easily damaged by debris flows (Hu et al. 2012). For this reason, it is important to analyze potential damage of residential buildings to debris flow hazards. A quantifiable integrated approach of hazard and risk management is becoming standard practice in risk reduction management (Fell and Hartford 1997; Duzgun and Lacasse 2005). Such quantitative assessment should include the expected losses as the product of the hazard with a given magnitude, the costs of the elements at risk, and the vulnerability (Uzielli et al. 2008).

The physical vulnerability is commonly expressed as the degree of loss or damage to a given element within the area affected by the hazard. Physical vulnerability is a representation of the expected degree of loss and is quantified on a scale of 0 (no damage) to 1 (total destruction) (Fell et al. 2005). Thus, vulnerability assessment requires an understanding of the interaction between the hazard and the exposed element. This interaction can be expressed using vulnerability curves (Quan Luna et al. 2011).

There have been a number of reports and studies on physical vulnerability (Fuchs et al. 2007; Haugen and Kaynia 2008; Quan Luna et al. 2011; Jakob et al. 2012; Papathoma-Köhle et al. 2012, 2015; Totschnig and Fuchs 2013). Fuchs et al. (2007) derived an empirical intensity–vulnerability relationship based on data from a debris flow event in the Austrian Alps. Haugen and Kaynia (2008) proposed a model for assessing the vulnerability of structures to the impact of debris flows by referring to HAZUS damage state probabilities and tested it by applying to the debris flow events of May 1998 in Sarno area. Quan Luna et al. (2011) obtained three different empirical vulnerability curves as functions of the depth of the debris flow, the impact pressure, and the kinematic viscosity via numerical modeling and reported a physical damage investigation of the Selvetta debris flow event that occurred in the central part of Valtellina Valley, Northern Italy. Jakob et al. (2012) defined four damage categories, from minor sedimentation to complete destruction, and related them with an intensity index represented by the impact force of the debris flow. Papathoma-Köhle et al. (2012, 2015) and Totschnig and Fuchs (2013) carried out a study for the uncertainty assessment in the methodological stage of vulnerability curve. They also suggested new documentation form for damage assessment to improve the vulnerability curve.

Few studies have been made on the vulnerability assessment of a building due to debris flow in spite of the possibility to provide useful information on management of vulnerable areas, prioritization of national disaster management policies, and future city planning. Therefore, this study aims to generate physical vulnerability curves essential for risk assessment. To this end, this study analyzes the intensity of debris flow and building damages through field survey data, spatial data, and empirical formulas.

In this study, a total of 25 buildings damaged in 11 debris flow events were investigated via extensive detailed field surveys to determine the characteristics and patterns of building damage. The physical vulnerability was obtained from the relationship between the degree of building damage and the intensity of the debris flow events. The intensity of the 11 debris flow events was calculated from empirical formulas. Three different empirical vulnerability curves were obtained, which are functions of the debris flow depth, flow velocity, and impact pressure, separately for different structural types of buildings. The resulting physical vulnerability values provide useful information for risk management and urban planning.

2 Study area

Many debris flow disasters have occurred in South Korea due to typhoons and heavy rainfall. Several debris flow disasters occurred throughout the country due to concentrated heavy rainfall between July and August, 2011, and there were many casualties, with much loss of property. Eleven study areas in which casualties and damage to property occurred were selected, as shown in Fig. 1. Figure 2 shows the average monthly rainfall at the

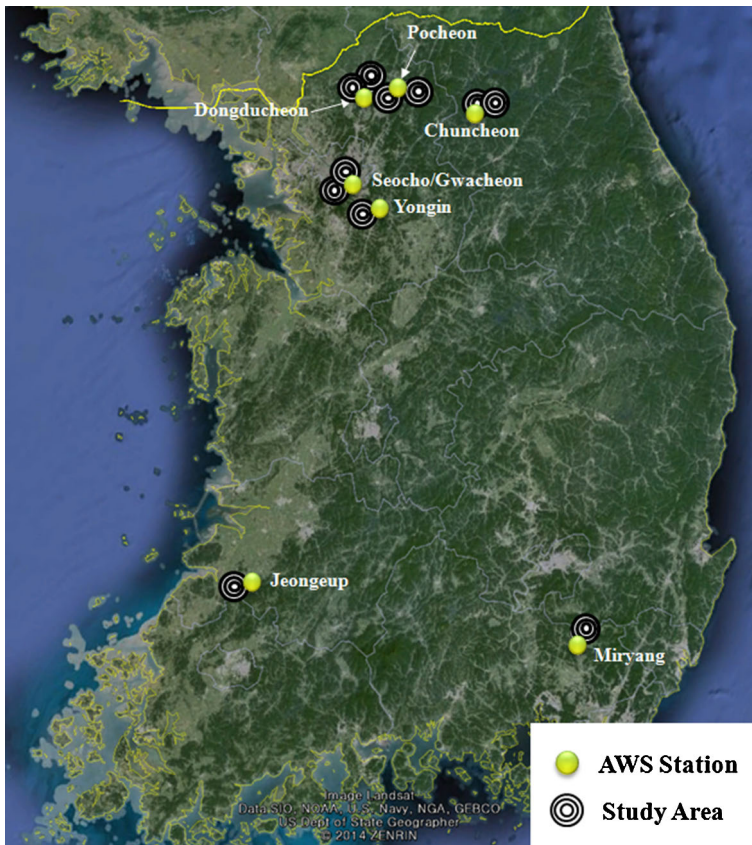


Fig. 1 Study area, showing the locations of the debris flow events, i.e., Miryang, Yongin, Pocheon I, Pocheon S, Dongducheon H, Gwacheon, Seocho, Dongducheon S, Chuncheon I, Chuncheon J, Jeongeup, as well as the AWS observation points

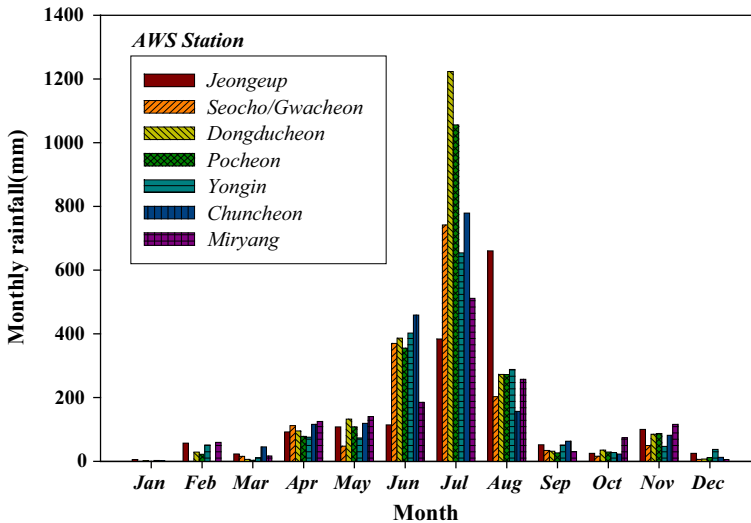


Fig. 2 Average monthly rainfall in 2011

corresponding sites in 2011. These average monthly rainfall data were obtained from the nearby automatic weather system (AWS) stations operated by the Korea meteorological administration. The precipitation was concentrated in the period from June to August. A cumulated precipitation of 1390 mm was measured from June to August, which corresponds to 76 % of the total annual rainfall, and 43 % of the total annual rainfall occurred in July. Among 11 debris flow disasters, 10 disasters occurred during heavy rainfall in July and 1 disaster in August, 2011.

Table 1 lists a summary report of the 11 debris flow disasters including the occurrence date, number of casualties, damage to property of the debris flows, soil type, characteristic of downstream areas, and the initiation area of debris flow occurred. With the exception of sites A and K, the debris flow disasters occurred between 27 and 28 July, 2011. During this period, extreme rainfall occurred in the central region of South Korea, and more than 500 mm fell during 3 days (KMA 2011). As shown in Fig. 1, it is found that debris flow disaster areas are concentrated in central districts than in southern regions of South Korea. In addition, the devastated areas due to 11 debris flow events were investigated to the rural area, residential area, or factory area. At sites I and J, 13 people were killed and 24 were injured. At site C, the sediment blocked part of the second floor of a three-story building that was composed of five households on the first floor. Because of this, three people were killed and one was injured. In particular, it is found that high casualties were appeared in residential building.

NDMI (2012) reported that the mountain crust in Korea is made up of 40 % metamorphic rock, 35 % granite rock, and 25 % sedimentary rock. As given in Table 1, eight debris flow events were occurred in weathered metamorphic soil and three events in weathered granite soil. It indicates that mountainous slope consisted of weathered metamorphic soil is more vulnerable to debris flow than weathered granite soil slope. Chae et al. (2007) also reported that slope disaster frequency is the highest in weathered metamorphic soil in Korea. In most cases, the initiation areas of the debris flows had a circular failure form, which developed into a debris flow due to the heavy rainfall. Most of the initiation

Table 1 Summary of the debris flow events

Site	Date ^a	Casualties ^a	Damage to property ^a	Soil type ^b	Characteristic of downstream area	Initiation area of the debris flow
Location	Note					
Miryang	July 09, 2011	Deaths: 4 Injured: 4	4 Residential buildings Several cars	Weathered granite soil	Rural area (village level)	Forest road
Yongin	July 27, 2011	Deaths: 1	2 Residential buildings	Metamorphic soil	Outskirts of a city	Tomb
Pocheon I	July 27, 2011	Deaths: 3 Injured: 1	3 Story building 2 Residential buildings	Weathered granite soil	Urban residential area	Construction temporary road
Pocheon S	July 27, 2011	Deaths: 1 Injured: 1	2 Pensions	Metamorphic soil	Accommodations region	–
Dongducheon H	July 27, 2011	Deaths: 1	1 Factory building	Metamorphic soil	Factory area	–
Gwacheon	July 27, 2011	Deaths: 1	3 Residential buildings Several cars	Metamorphic soil	Residential area	Automobile road
Secho	July 27, 2011	Deaths: 5	High-rise apartment (damage to the fifth floor)	Metamorphic soil	Downtown area (high-rise apartment area)	Military facility
Dongducheon S	July 28, 2011	Deaths: 4	2 Residential buildings	Metamorphic soil	Factory area	–
Chuncheon	July 28, 2011	Deaths: 13 Injured: 24	5 Residential buildings 1 Pension	Metamorphic soil	Accommodations and restaurants region	Military facility and forest road
Chuncheon	July 28, 2011					
Jeongseup	August 09, 2011	Deaths: 1 Injured: 1	1 Residential building	Weathered granite soil	Rural area (village level)	–

^a Field survey data in 2011, National Disaster Management Institute (NDMI)

^b The geological information system of Korea Institute of Geoscience and Mineral Resources (KIGAM)

areas of the debris flows were located in forest roads, temporary construction roads, tombs, mounds, or military facilities. This indicates that human activities influence the magnitude and frequency of debris flows.

3 Methodology

The physical characteristics of debris flows were analyzed for the 11 debris flow events between July and August, 2011. A variety of data on the debris flow characteristics were obtained from field surveys, topographic map (2010), aerial photographs (2011), and field reports to analyze the characteristics of the affected regions. Figure 3 shows aerial photographs of the study areas including the failed or scoured areas, depositional area, and catchment areas of each debris flow disaster. The characteristics of the damaged buildings for each debris flow event were also investigated. The degree of damage to the buildings was determined from a comprehensive analysis of field survey data, photographs, and field reports from the scenes.

The procedure followed in the presented study is shown in Fig. 4. Overall, the methodological procedure of this study is divided into three steps. In the step 1, physical characteristics (mobility index, volume, catchment area, and peak discharge) of debris flows were analyzed based on field survey and spatial data. The intensity of debris flow (flow depth, flow velocity, and impact pressure) was also calculated through the physical characteristics of debris flows and empirical formulas. In the step 2, the characteristics of damage according to the structural type of a building were investigated using the photographs of building damage and field survey data. A value of vulnerability index was assigned according to degree of damage to the building. Finally, vulnerability curves were calculated based on the relationship between the intensity of debris flow obtained from step 1 and building damage obtained from step 2.

3.1 Physical characteristics of the debris flows

Debris flow can be divided into hillslope debris flow and channelized debris flow. Hillslope debris flow has a smaller size, a short travel distance, or a faster moving speed as compared to channelized debris flow. In order to understand the type of debris flow, the mobility index of each study area was analyzed. The mobility index is the ratio of the horizontal distance L between the source area and distal limit of the deposit to the difference in height ΔH and corresponds to the mobility of gravity-driven mass flows (Iverson 1997). A larger ratio $L/\Delta H$ corresponds to a greater mobility of the debris flow.

The debris flow volume V is one of the most important parameters affecting the hazard's destructive potential. It is difficult to estimate the debris flow volume accurately because it depends on several factors such as the rainfall, catchment area, slope angle, topographic characteristics, and soil depth. In this study, the total volume was calculated by combining the measured area (A) of the failed/scoured region and its average thickness (h), which were determined from field surveys and aerial photograph (2012), as shown in Fig. 3. The estimated volume ($V = A \times h$) represents the magnitude of each debris flow event.

Physical characteristics of debris flows such as peak discharge, flow velocity, and impact pressure can be estimated empirically (Zanchetta et al. 2004). The characteristics assessed in this way give only a rough approximation of the actual behavior of debris flows, but they can be reasonably assumed for flow parameterization (Pierson 1985; Costa

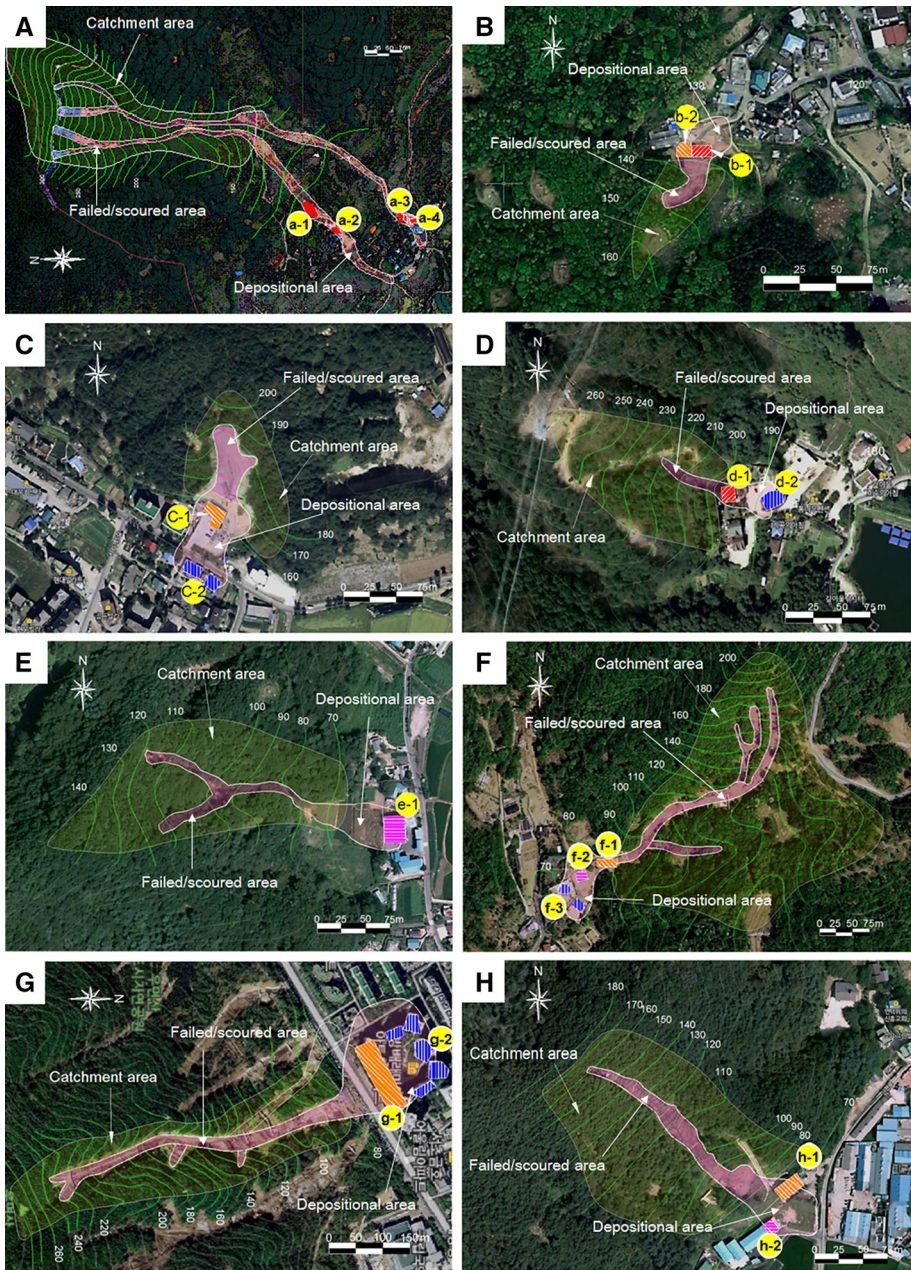


Fig. 3 Contour and debris flow overlaid in aerial photographs: **a** Miryang, **b** Yongin, **c** Pocheon I, **d** Pocheon S, **e** Dongducheon H, **f** Gwacheon, **g** Seocho, **h** Dongducheon S, **i** Chuncheon I, **j** Chuncheon J, and **k** Jeongeup

1997). The peak discharge Q_p can be assessed using empirical relationships between peak discharge of a debris flow and V (Hung et al. 1984; Mizuyama et al. 1992; Rickenmann 1999). In this study, an empirical formula proposed by Rickenmann (1999) was used to

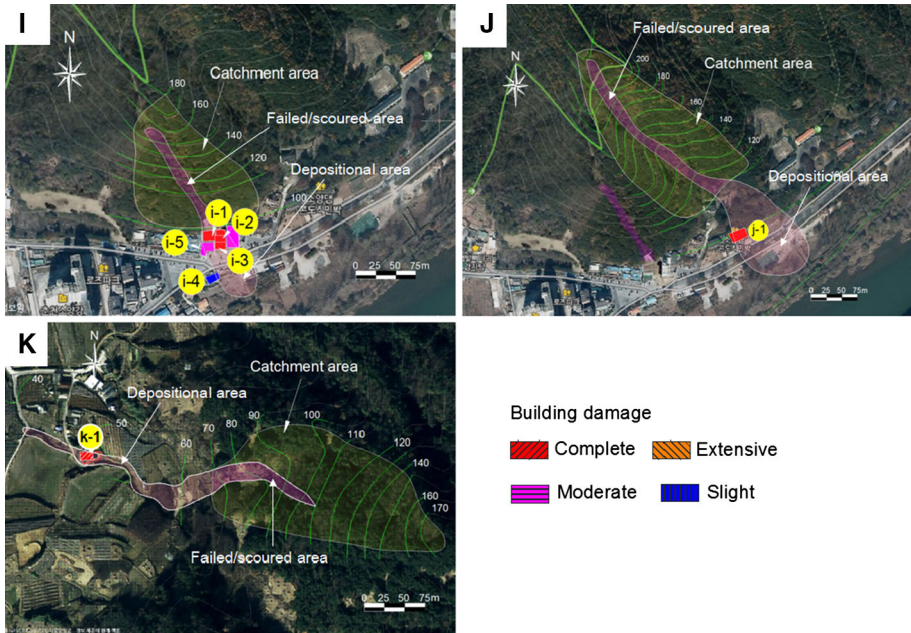


Fig. 3 continued

obtain the value of the peak discharge and flow velocity, because the variables included in the equation are easy to obtain, and the result of application in the study areas showed a good correlation.

$$Q_p = 0.1V^{0.833} \tag{1}$$

where V is the total volume of the debris flow.

The debris flow velocity at peak discharge was estimated using the following empirical relation (Rickenmann 1999):

$$v = 2.1Q_p^{0.33}S^{0.33} \tag{2}$$

where Q_p is the peak discharge calculated using Eq. 1, and S is the local slope (defined here as the ratio of the change in elevation (Δh) to the horizontal distance (L), $S = \Delta h/L$, which can be calculated using the contour and debris flow overlaid in aerial photographs shown in Fig. 3).

3.2 Impact pressure

The impact pressure of the debris flow, or flow impact on obstacles, mainly consists of dynamic overpressure and hydrostatic pressure. These forces depend on the peak discharge, velocity, volume, sediment–water ratio, and grain-size distribution of debris flow (Zanchetta et al. 2004). By adding the dynamic overpressure and the hydrostatic pressure, the average impact pressure can be obtained as follows (Zanchetta et al. 2004):

$$P_t = (1/2)\rho_{df}gh + \rho_{df}v^2 \tag{3}$$

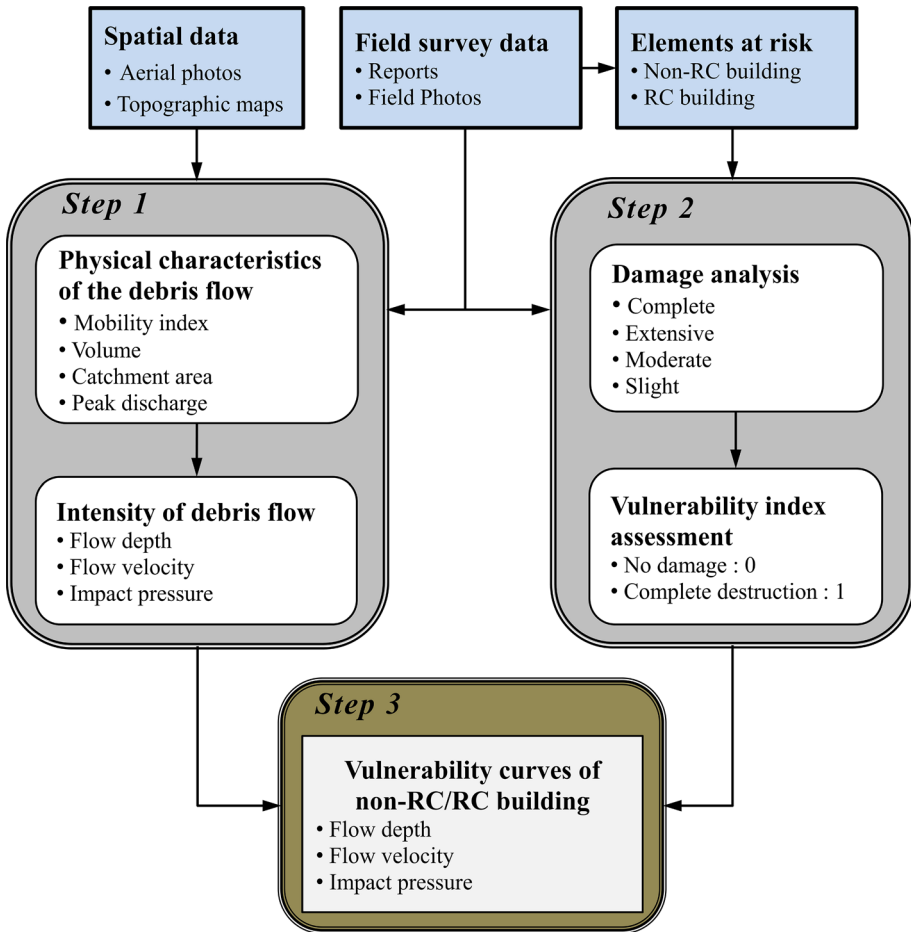


Fig. 4 Flowchart of the methodology applied in this study

where ρ_{df} is the mean density of the material, v is the flow velocity, h is the flow depth, and g is the acceleration due to gravity. The first term in Eq. 3, $(1/2)\rho_{df}gh$, is the mean hydrostatic pressure component, and the second term, $\rho_{df}v^2$, is the dynamic overpressure component.

The density of a debris flow is in the range 1500–2500 kg m⁻³, and typically 2000–2200 kg m⁻³ (e.g., Curry 1966; Pierson 1981, 1985; Okuda et al. 1980; Li and Luo 1981; Li et al. 1983; Zhang 1993; Iverson 1997). Hu et al. (2012) reported a density of 2000 kg m⁻³ by analyzing sediment samples taken from debris flow deposits 2 days after the event in Zhouqu, Western China. In this work, we assumed that the density of the debris flows was 2000 kg m⁻³. The impact pressure was calculated using the calculated flow velocity and the depth of the flow. The flow depth is the sediment height on damaged buildings. The depth of the debris flow can be obtained from the field surveys or calculation. The flow depth was estimated by using the residues on the wall of a building, obtained through field survey data (field survey and photographs of damaged building). In addition, the depth of debris flow can also be calculated through the relationship between

the area of deposition zone at the location of the damaged building and the total volume of debris flow. Field surveys and photographs of each debris flow event were obtained within 3 days after the debris flow occurred.

3.3 Building damage

The degree of damage to buildings was determined from a comprehensive analysis of field survey data, photographs, and reports. To evaluate building damage due to debris flows, it is necessary to establish a system of damage classification. The degree of damage to buildings was categorized as follows: complete destruction, extensive damage, moderate damage, and slight damage. This classification scheme follows that proposed by Leone et al. (1996) and Hu et al. (2012). These four categories of degree of damage are similar to the damage states defined in the HAZUS earthquake methodology (Kircher et al. 2006).

The 25 buildings that were damaged during the debris flow events were investigated in detail to analyze the characteristics and patterns of damage. The degree of the damaged building in devastated areas was determined from damage of exterior wall of a building, crack in wall, loss of parts of external and internal wall, flooding of internal rooms, or damage of main column of a building.

4 Results and discussion

4.1 Characteristics of the debris flows

Table 2 shows physical characteristics of the 11 debris flow disasters. These events have a mobility index ($L/\Delta H$) between 3.4 and 6.4. The variation in the mobility index was similar to that reported by Iverson (1997) for small-volume debris flows originating from landslides. These mobility index data were also in agreement with data for volcaniclastic debris flow events that occurred in southern Campania during May 5–6, 1998, and in preceding years (Calcaterra et al. 1999; Pareschi et al. 2002).

The total volume of the debris flows was in the range 4.76×10^2 – 4.55×10^4 m³. The catchment area of the debris flow regions was in the range 2.53×10^3 – 9.64×10^4 m². The peak discharge was calculated using Eq. 1; Q_p was in the range 15.6–759.3 m³/s and was largest at site Seocho. Jakob (2005) classified the scale of debris flows according to Q_p , and using this system, the debris flows discussed here are grade 3, which corresponds to the destruction of large buildings, damage to concrete bridges and piers, or damage to highways and pipelines. As given in Table 2, the average slope was in the range 0.22–0.41, the slope of the transportation zone was in the range 0.32–0.51, and the slope of the deposition zone was in the range 0.1–0.2. The results indicate that the deposition of the debris flow materials started when the slope became less than 0.2. Overall, maximum flow velocity was in the range 3.8–14.9 m/s.

Figure 5 shows the relationship between peak discharge and maximum flow velocity, where the results of a number of previous studies are also shown for comparison. The maximum flow velocity increased with increasing peak discharge. The maximum flow velocity shows a strong positive correlation with the peak discharge, and the relationship between these two quantities is in good agreement with the data reported by Scheidl and Rickenmann (2011), Suwa et al. (2003), and Cui et al. (1999).

Table 2 Physical characteristics of the debris flows

Region	$L/\Delta H$	Catchment area (m ²)	Volume [V (m ³)]	Peak discharge [Q_p (m ³ s ⁻¹)]	Local slope (S)		Maximum flow velocity [v (m/s)]	
					Transportation part			Average
					Deposition part	Average		
Miryang	4.3	7.59×10^4	1.16×10^4	136.0	0.49	0.12	10.5	
Yongin	3.4	2.53×10^3	4.31×10^2	15.6	0.37	0.20	3.8	
Pocheon I	5.0	9.51×10^3	4.33×10^3	107.0	0.49	0.12	8.4	
Pocheon S	3.2	1.27×10^4	4.76×10^2	17.0	0.51	0.15	4.5	
Dongducheon H	5.7	2.76×10^4	2.10×10^3	65.8	0.29	0.11	5.9	
Gwacheon	4.4	9.64×10^4	3.32×10^3	85.7	0.36	0.11	7.4	
Secho	4.4	8.55×10^4	4.55×10^4	759.3	0.32	0.13	14.9	
Dongducheon S	3.1	3.27×10^4	2.62×10^3	70.3	0.46	0.19	7.4	
Chuncheon_1	3.8	1.74×10^4	1.84×10^3	52.4	0.44	0.10	6.5	
Chuncheon_2	3.8	3.83×10^4	1.66×10^4	327.9	0.43	0.10	12.8	
Jeongsup	6.4	2.98×10^4	2.34×10^3	64.1	0.34	0.10	6.7	

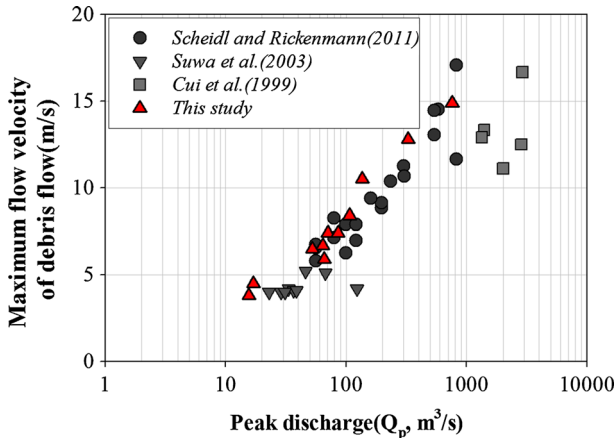


Fig. 5 Maximum flow velocity as a function of the peak discharge

Table 3 lists the intensities of the debris flows, including the depth, velocity, and impact pressure on the 25 buildings in the disaster areas. The impact pressure calculated using Eq. 3 was in the range 8.5–201.5 kPa, with an average of 53.2 kPa.

4.2 The characteristics of building damage

Table 3 lists the description of damage to buildings due to the intensities of debris flow. The structural type of the building was assigned according to the HAZUS building classification scheme, whereby a total of 36 items are classified according to the structure type, material, and height of the building. In this work, buildings are classified into the following four structural types: masonry, RC frame, wooden frame, and light steel frame. For the same structural type of the damaged building, the higher the intensity of the debris flow (such as the impact pressure, velocity, and depth) usually resulted in the more severe damage of the buildings. Damage depends not only on the intensities of the debris flow, but also on the structural strength and the orientation of the buildings. The chance of casualties was higher in wooden buildings or masonry buildings than in reinforced concrete (RC) buildings. It is noted that the damage to buildings depends strongly on the structural type of the building. Compared with masonry buildings, which have little resistance to horizontal thrust, buildings with RC frames can resist much larger impacts due to debris flows.

Figure 6 shows photographs of the damaged buildings taken at the 11 debris flow disaster sites. Most of the masonry buildings were seriously damaged or completely destroyed. The brick buildings a-1 and b-1 were completely destroyed by the debris flows (see Fig. 6). The red arrows in Fig. 6 indicate the direction of debris flow events. The majority severe damage occurred to buildings that were located around the main streamline of the debris flow and impacted by proximal debris flows, where most of the mass and energy are concentrated.

4.3 Relationship between impact pressure and building damage

The impact pressure is an important index for assessing the damage to building due to debris flows. Impact pressure calculated using Eq. 3 contains information such as the

Table 3 Intensities of the debris flows and description of the damage

Building no.	Intensities of debris flow			Description of the damage to buildings		
	Flow depth [d (m)]	Flow velocity [v (m/s)]	Impact pressure [P (kPa)]	Description	HAZUS label	Damage scale
a-1	1.33	3.4	36.4	Brick masonry/low rise	URML	Complete
a-2	0.97	3.3	31.2	Wood/low rise	W1	Complete
a-3	1.09	3.5	35.3	Wood/low rise	W1	Complete
a-4	0.99	3.5	34.4	Brick masonry/low rise	URML	Complete
b-1	2.70	3.5	51.5	Brick masonry/low rise	URML	Complete
b-2	0.52	2.4	16.6	Brick masonry/low rise	URML	Extensive
c-1	3.89	6.0	110.1	RC frame/low rise	C2L	Extensive
c-2	1.09	2.4	22.6	RC frame with unreinforced masonry infill walls/low rise	C3L	Slight
d-1	2.71	3.6	53.1	Wood/low rise	W1	Complete
d-2	0.40	2.3	14.3	Wood/low rise	W1	Slight
e-1	0.84	3.5	32.6	RC frame with unreinforced masonry infill walls/low rise	C3L	Moderate
f-1	5.84	4.5	98.4	RC frame/low rise	C2L	Extensive
f-2	1.57	4.7	59.6	RC frame with unreinforced masonry infill walls/low rise	C3L	Moderate
f-3	0.59	3.8	35.2	RC frame with unreinforced masonry infill walls/low rise	C3L	Slight
g-1	5.80	8.5	201.5	RC frame/high rise	C2H	Extensive
g-2	1.54	3.7	43.0	RC frame/high rise	C2H	Slight
h-1	2.88	6.0	100.4	RC frame with unreinforced masonry infill walls/low rise	C3L	Extensive
h-2	0.83	2.9	24.6	Light steel frame	S3	Moderate
i-1	3.22	4.2	66.5	Brick masonry/low rise	URML	Complete
i-2	1.98	3.7	46.2	Brick masonry/low rise	URML	Complete
i-3	1.44	3.5	38.0	Brick masonry/low rise	URML	Complete
i-4	0.66	1.0	8.5	Brick masonry/low rise	URML	Slight
i-5	1.44	2.3	24.7	Brick masonry/low rise	URML	Moderate
j-1	3.23	6.6	118.8	Brick masonry/low rise	URML	Complete
k-1	0.71	3.2	27.3	Brick masonry/low rise	URML	Complete

debris flow depth, velocity, and density of material. Different types of building structures suffer different degrees of damage under the same debris flow impact due to their different structural strengths. For this reason, we used a quantitative indication of the degree of damage to buildings depending on the impact pressure of the debris flow and structural types of the building.



Fig. 6 Photographs showing buildings damaged due to debris flows in **a** Miryang, **b** Yongin, **c** Pocheon I, **d** Pocheon S, **e** Dongducheon H, **f** Gwacheon, **g** Seocho, **h** Dongducheon S, **i** Chuncheon I, **j** Chuncheon J, and **k** Jeongseup

To determine the degree of damage depending on the structural type, the damaged buildings investigated were divided into two types: RC frame and non-RC frame, where non-RC frame structures include masonry, wooden frame, and light steel frame structures.

Table 4 lists the relationship between the damage to the buildings and the impact pressure of the debris flow. With the non-RC buildings, complete destruction occurred with an impact pressure of greater than 30 kPa, extensive and moderate damage occurred with impact pressures in the range 15–30 kPa, and slight damage occurred with impact pressures of less than 15 kPa. For the RC buildings, extensive damage occurred with impact pressures greater than 100 kPa, moderate damage with impact pressures in the range 35–100 kPa, and slight damage at the impact pressures below 35 kPa. Impact pressures of debris flows that led to slight damage to RC buildings can result in complete destruction of non-RC buildings. The degree of damage to buildings depends strongly on the type of structure, as well as the impact pressure of the debris flow.

Table 4 Classification of damage to buildings due to the debris flows

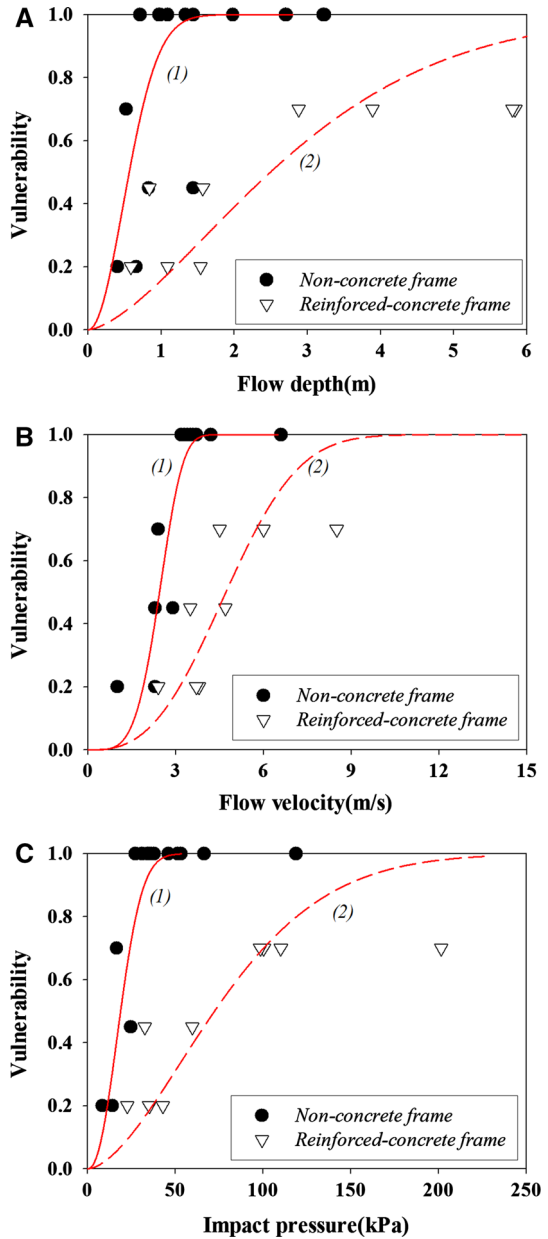
Damage class	Damage description	Vulnerability (used value)	Impact pressure (kPa)	
			Non-RC frame	RC frame
Complete	Partly or totally destroyed, evacuation necessary, complete reconstruction	0.8–1.0 (1.0)	>30	–
Extensive	Partly destroyed, loss of parts of external and internal walls, evacuation necessary, reconstruction of destroyed parts	0.6–0.8 (0.7)	15–30	>100
Moderate	Cracks in the wall, stability unaffected, reparation not urgent, flooding of the internal rooms and damage to the furnishing	0.3–0.6 (0.45)		35–100
Slight	Slight non-structural damage, stability not affected, damage to furnishings or fittings	0.1–0.3 (0.2)	0–15	0–35

4.4 Vulnerability curves

The range of damage to the buildings makes it possible to assess the vulnerability using a vulnerability curve that relates the intensity of debris flow with the degree of damage. In this work, vulnerability curves were estimated using the degree of damage to the buildings (Tables 3, 4) coupled with intensities of the debris flow events (Table 3). An average value of vulnerability index corresponding to degree of damage to the building was used in vulnerability curves. This allowed us to develop the vulnerability curves as shown in Fig. 7. Three different empirical vulnerability curves were obtained, which were function of debris flow depth (see Fig. 7a), flow velocity (see Fig. 7b), and impact pressure (see Fig. 7c). The vulnerability for the RC and non-RC buildings is different due to their different structural strengths of the buildings. The vulnerability curves of the non-RC buildings increased more rapidly with increasing in flow depth, flow velocity, and impact pressure than those of the RC buildings. The intensity of debris flow corresponding to a slight damage to RC frame buildings can result in the complete destruction of non-RC buildings. As the intensity of debris flow increases, the difference of the vulnerability index between non-RC and RC buildings increases. In order to reach the vulnerability index of 1 in non-RC building, debris flow depth of 1.44 m, flow velocity of 3.8 m/s, and impact pressure of 44.5 kPa are required. On the other hand, debris flow depth of 8.6 m, flow velocity of 9.4 m/s, and impact pressure of 222 kPa are required for the RC building. The intensity of debris flow corresponding to a slight damage to RC frame buildings can result in the complete destruction of non-RC buildings.

Figure 8 shows the vulnerability function as a function of impact pressure for the non-RC buildings, as well as that reported by Quan Luna et al. (2011) and Barbolini et al. (2004). The three datasets are in good agreement. Quan Luna et al. (2011) proposed vulnerability curves by numerical modeling and reported a physical damage investigation of the Selvetta debris flow event that occurred in the central part of Valtellina Valley, Northern Italy. Barbolini et al. (2004) proposed a linear vulnerability curve, which was developed from avalanche data for West Tyrol, Austria. This indicates that the non-RC

Fig. 7 Debris flow vulnerability curves **a** as a function of the flow depth, **b** as a function of the of flow velocity, and **c** as a function of the of impact pressure



buildings damaged by the 11 debris flows have a similar structural resistance as those studied by Quan Luna et al. (2011) and Barbolini et al. (2004).

Nonlinear regression analysis was carried out to relate the vulnerability to the intensity of the debris flows using an analytic expression. To nonlinear regression analysis, a sigmoid function having an “S” shape was used. This function is an asymptote from a small value close to zero to a certain finite value. Table 5 lists the vulnerability functions for the

Fig. 8 Comparison of the vulnerability curve proposed by Quan Luna et al. (2011) and Barbolini et al. (2004) and the vulnerability curve calculated from this research

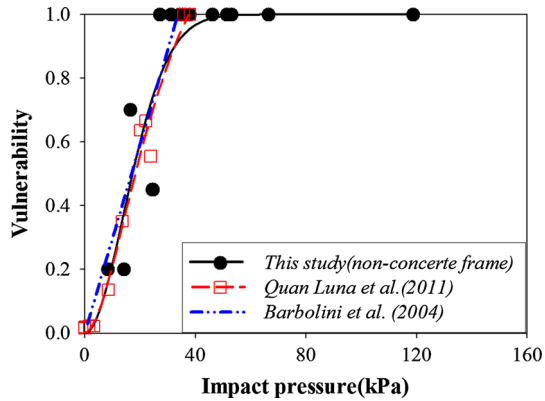


Table 5 Vulnerability functions for the different types of building structures

Intensity parameter	Vulnerability function	
	Non-RC frame (1)	RC frame (2)
Flow velocity [v (m/s)]	$V = 1 - e^{(-0.0140 \times v^{4.368})}$	$V = 1 - e^{(-0.0094 \times v^{2.775})}$
Flow depth [d (m)]	$V = 1 - e^{(-2.2072 \times d^{2.019})}$	$V = 1 - e^{(-0.1703 \times d^{1.537})}$
Impact pressure [P (kPa)]	$V = 1 - e^{(-0.0010 \times p^{2.227})}$	$V = 1 - e^{(-0.0005 \times p^{1.690})}$

RC and non-RC structural types. The intensity parameters used to calculate the vulnerability curves were the flow depth, flow velocity, and impact pressure calculated for the 11 debris flow events.

The suggested vulnerability functions have many limitations because the damaged building in this study was simply divided into two types (RC building and non-RC building). Only 25 damaged buildings from 11 debris flow events were used in development of vulnerability curves. Degree of damage to the buildings depends not only on structural types of building but also on shape, direction, position, etc. To practical application, there is a need for a more detail classification of damaged buildings with establishment of database regarding debris flow events. Nevertheless, the presented approach attempts to propose a quantitative method to estimate the vulnerability of an exposed element to a debris flow. The resulting physical vulnerability curves can be used to estimate the structural resistance of buildings to debris flow events.

5 Conclusions

The physical characteristics of debris flows were evaluated based on data from 11 debris flow events that occurred in July and August, 2011 in South Korea. A total of 25 damaged buildings were investigated in detail to determine the characteristics and patterns of the damage to buildings resulting from debris flows. Three different vulnerability curves were obtained as functions of the debris flow depth, flow velocity, and impact pressure, for two structural types of building.

Most of the masonry buildings were completely destroyed or seriously damaged, which is attributed to a greater vulnerability of brick buildings to lateral loads. With the non-RC buildings, complete destruction occurred with impact pressures of greater than 30 kPa. For the case of RC buildings, slight damage occurred with impact pressures of less than 35 kPa. The impact pressure of debris flow corresponding to slight damage to an RC building resulted in complete destruction of non-RC buildings. The vulnerability curves of the non-RC buildings increased with increasing flow depth, flow velocity, and impact pressure more rapidly than those of the RC buildings. Different structural types of buildings had different vulnerability curves and damage patterns.

The proposed vulnerability curves have limitations because only 25 damaged buildings from 11 debris flow events were used. For more accurate vulnerability assessment, a further study is needed based on database with a more debris flow events. Vulnerability index of a building due to the impact of the debris flow is difficult to estimate because it depends on various characteristics of buildings such as the structural type, shape, position, direction, and number of windows. Despite the disadvantage and limitations of the present study, the presented approach attempts to propose a method to estimate the vulnerability of two structural types of building.

Acknowledgments This research was supported by the Public Welfare and Safety Research Program through the National Research Foundation of Korea (NRF), funded by the Ministry of Science, ICT, and Future Planning (Grant No. 2012M3A2A1050977), a Grant (13SCIPS04) from Smart Civil Infrastructure Research Program funded by Ministry of Land, Infrastructure and Transport (MOLIT) of Korea government and Korea Agency for Infrastructure Technology Advancement (KAIA) and the Brain Korea 21 Plus (BK 21 Plus).

References

- Barbolini M, Cappabianca F, Sailer R (2004) Empirical estimate of vulnerability relations for use in snow avalanche risk assessment. In: Brebbia C (ed) Risk analysis IV. WIT Press, Southampton, pp 533–542
- Calcaterra D, Parise M, Palma B, Pelella L (1999) The May 5th 1998, landsliding event in Campania (southern Italy): inventory of slope movements in the Quindici area. In: Yagi N, Yamagami T, Jiang J (eds) Proceedings of the international symposium on slope stability engineering, IS, Shikoku '99, Matsuyama, Shikoku, November 8–11, 1999. Balkema, Rotterdam, pp 1361–1366
- Chae BG, Lee SH, Song YS, Cho YC, Seo YS (2007) Characterization on the relationships among rainfall intensity, slope angle and pore water pressure by a flume test: in case of gneissic weathered soil. *J Eng Geol* 17:57–64 (in South Korea)
- Costa JE (1997) Hydraulic modeling for lahar hazards at Cascades volcanoes. *Environ Eng Geosci* 3:21–30
- Cui P, Wei FQ, Li Y (1999) Sediment transported by debris flow to the lower Jiansha river. *Int J Sedim Res* 14(4):67–71
- Curry RR (1966) Observation of alpine mudflows in the Tenmile Range, central Colorado. *Geol Soc Am Bull* 77:771–776
- Duzgun HSB, Lacasse S (2005) Vulnerability and acceptable risk in integrated risk assessment framework. In: Hungr O, Fell R, Couture R, Eberhardt E (eds) Landslide risk management. Balkema, Rotterdam, pp 505–515
- Fell R, Hartford D (1997) Landslide risk management. In: Cruden D, Fell R (eds) Landslide risk assessment. Balkema, Rotterdam, pp 51–109
- Fell R, Ho KKS, Lacasse S, Leroi E (2005) A framework for landslide risk assessment and management. In: Hungr O, Fell R, Couture R, Eberhardt E (eds) Landslide risk management. Taylor & Francis, London, pp 533–541
- Fuchs S, Heiss K, Hubl J (2007) Towards an empirical vulnerability function for use in debris flow risk assessment. *Nat Hazards Earth Syst Sci* 7:495–506
- Haugen ED, Kaynia AM (2008) Vulnerability of structures impacted by debris flow. In: Chen Z, Zhang JM, Ho K, Wu FQ, Li ZK (eds) Landslides and engineered slopes. Taylor & Francis, London, pp 381–387
- Hu KH, Cui P, Zhang JQ (2012) Characteristics of damage to buildings by debris flows on 7 August 2010 in Zhouqu, Western China. *Nat Hazards Earth Syst Sci* 12:2209–2217

- Hungr O, Morgan GC, Kellerhals R (1984) Quantitative analysis of debris torrent hazard for design of remedial measures. *Can Geotech J* 21:663–677
- Iverson RM (1997) The physics of debris flows. *Rev Geophys* 35:254–296
- Jakob M (2005) A size classification for debris flows. *Eng Geol* 79:151–161
- Jakob M, Stein D, Ulmi M (2012) Vulnerability of buildings to debris flow impact. *Nat Hazards* 60:241–261
- Kircher CA, Whitman RV, Holmes WT (2006) HAZUS earthquake loss estimation methods. *Nat Hazards Rev* 7:45–59
- KMA (2011) Annual report 2011. Korea Meteorological Administration
- Leone F, Aste JP, Leroi E (1996) Vulnerability assessment of elements exposed to mass-movement: working toward a better risk perception. In: Senneset K (ed) *Landslides*, vol 1. A.A. Balkema, Amsterdam, pp 263–269
- Li J, Luo D (1981) The formation and characteristics of mudflow and flood in the mountain area of the Dachao river and its prevention. *Z Geomorphol NF* 25:470–484
- Li J, Yuan J, Bi C, Luo D (1983) The main features of the mud flow in Jiang-Jia Ravine. *Z Geomorphol NF* 27:325–341
- Mizuyama T, Kobashi S, and Ou G (1992) Prediction of debris flow peak discharge. In: *International symposium interpraevent*, Bern, pp 99–108
- Nadim F, Kjekstad O (2009) Assessment of global high-risk landslide disaster hotspots. In: Sassa K, Canuti P (eds) *Disaster risk reduction*. Springer, Berlin, pp 213–222
- NDMI (2012) Unsaturated characteristics and steep-slope risk evaluation of weathered metamorphic soil testbeds. National Disaster Management Institute, pp 17–41
- Okuda S, Okunishi K, and Suwa H (1980) Observation of debris flow at Kamikamihori Valley of Mt. Yakedake. In: Okuda S, Suzuki T, Hirano K, Okunishi M, Suwa H (eds) *Third meeting of IGU commission on field experiments in geomorphology, Japan*, pp 116–139
- Papathoma-Köhle M, Keiler M, Totschnig R, Glade T (2012) Improvement of vulnerability curves using data from extreme events: a debris-flow event in South Tyrol. *Nat Hazards* 64:2083–2105
- Papathoma-Köhle M, Zischg A, Fuchs S, Glade T, Keiler M (2015) Loss estimation for landslides in mountain areas—an integrated toolbox for vulnerability assessment and damage documentation. *Environ Model Softw* 62:156–169
- Pareschi MT, Santacroce R, Sulpizio R, Zanchetta G (2002) Volcaniclastic debris flow in the Clanio Valley (Campania, Italy): insights for the assessment of hazard potential. *Geomorphology* 43:219–231
- Pierson TC (1981) Dominant particle support mechanisms in debris flows at Mt. Thomas, New Zealand, and implication for flow mobility. *Sedimentology* 28:49–60
- Pierson TC (1985) Initiation and flow behavior of the 1980 Pine Creek and Muddy River lahars, Mt. St. Helens, Washington. *Geol Soc Am Bull* 96:1056–1069
- Quan Luna B, Blahut J, van Westen CJ, Sterlacchini S, van Asch TWJ, Akbas SO (2011) The application of numerical debris flow modelling for the generation of physical vulnerability curves. *Nat Hazards Earth Syst Sci* 11:2047–2060
- Rickenmann D (1999) Empirical relationships for debris flows. *Nat Hazards* 19(1):47–77
- Sassa K, Fukuoka H, Wang FW (1997) Mechanism and risk assessment of landslide-triggered-debris flows: Lesson from the 1996.12.6 Otari debris flow disaster, Nagano, Japan. In: Cruden D, Fell R (eds) *Landslide risk assessment*. A.A. Balkema, Rotterdam, pp 347–356
- Scheidl C, and Rickenmann D (2011) TopFlowDF—a simple GIS based model to simulate debris-flow runout on the fan. In: *5th international conference on debris-flow hazards mitigation: mechanics, prediction and assessment*, Padua, Italy, 14–17 June 2011, pp 253–262
- Suwa H, Akamatsu J, Nagai Y (2003) Energy radiation by elastic waves from debris flows. In: Rickenmann D, Wiecezorek G (eds) *Proceedings of the 3rd international conference on debris-flow hazards mitigation: mechanics, prediction, and assessment*. Balkema, Amsterdam, pp 895–904
- Totschnig R, Fuchs S (2013) Mountain torrents: quantifying vulnerability and assessing uncertainties. *Eng Geol* 155:31–44
- Uzielli M, Nadim F, Lacasse S, Kaynia AM (2008) A conceptual framework for quantitative estimation of physical vulnerability to landslides. *Eng Geol* 102(3–4):251–256
- Van Westen CJ, Rengers N, Soeters R (2003) Use of geomorphological information in indirect landslide susceptibility assessment. *Nat Hazards* 30:399–419
- Zanchetta G, Sulpizio R, Pareschi MT, Leoni FM, Santacroce R (2004) Characteristics of May 5–6, 1998 volcaniclastic debris-flows in the Sarno area of Campania, southern Italy: relationships to structural damage and hazard zonation. *J Volcanol Geotherm Res* 133:377–393
- Zhang S (1993) A comprehensive approach to the observation and prevention of debris flows in China. *Nat Hazards* 7:1–23